

DR. BEHZAD JAVAHERI (Orcid ID : 0000-0001-7941-3104)

DR. GEORGE BOU-GHARIOS (Orcid ID : 0000-0002-9563-9418)

Article type : Full Length

Targeted inhibition of aggrecanases prevents articular cartilage degradation and augments bone mass in the STR/Ort spontaneous model of osteoarthritis

Ioannis Kanakis, PhD,¹ Ke Liu, PhD,¹ Blandine Poulet, PhD,¹ Behzad Javaheri, PhD,² Rob J van 't Hof, PhD,¹ Andrew A Pitsillides, PhD,² George Bou-Gharios, PhD^{1,*}

¹ Institute of Ageing and Chronic Disease, University of Liverpool, Liverpool, UK

² Comparative Biomedical Sciences, The Royal Veterinary College, London, UK

Running title: Blocking aggrecanases protects from OA and increases bone mass.

Address correspondence to Professor George Bou-Gharios, Institute of Ageing and Chronic Disease, Faculty of Health & Life Sciences, William Henry Duncan Building, 6 West Derby Street, L7 8TX, Liverpool, UK.

e-mail: ggharios@liverpool.ac.uk

© 2018 The Authors Arthritis & Rheumatology published by Wiley Periodicals, Inc. on behalf of American College of Rheumatology

This is an open access article under the terms of the Creative Commons Attribution-NonCommercial-NoDerivs License, which permits use and distribution in any medium, provided the original work is properly cited, the use is non-commercial and no modifications or adaptations are made.

Supported by the Arthritis Research UK (grants 20039 and 20581).

ABSTRACT

Background:

Cartilage destruction in osteoarthritis (OA) is mediated mainly by MMPs and ADAMTSs. The therapeutic candidature of targeting aggrecanases has not yet been defined in joints where spontaneous OA arises due to genetic susceptibility, without a traumatic or load-induced aetiology such as the STR/Ort mouse. Nor do we know the long-term effect of aggrecanase inhibition on bone.

Methods:

Using the STR/Ort spontaneously OA background, we have generated transgenic mice that overexpress [-1A]TIMP-3, either ubiquitously or conditionally in chondrocytes. [-1A]TIMP-3 is a variant of tissue inhibitor of metalloproteinase-3 (TIMP-3) that has an extra alanine at the N-terminus that selectively inhibits ADAMTSs, but not MMPs. We analysed a range of OA-related measures in all mice at 40 weeks of age.

Results:

Mice expressing high [-1A]TIMP-3 levels were protected against the development of the OA whilst low expressers were not. Interestingly, we also found that high levels of [-1A]TIMP-3 transgene overexpression resulted in raised bone mass particularly in females. This regulation of bone mass is, at least, partly direct as primary adult osteoblasts infected with [-1A]TIMP-3 *in vitro* show elevated rates of mineralisation.

Conclusions:

The results provide evidence that [-1A]TIMP-3-mediated inhibition of aggrecanases can protect from cartilage degradation in naturally occurring OA mouse model and highlight a novel role that aggrecanases' inhibition may play in increased bone mass.

Osteoarthritis (OA) is characterized by altered homeostasis of articular cartilage and abnormal bone formation. OA development is dependent on a balance between extracellular matrix (ECM) production and degradation. The proteolytic enzymes such as a disintegrin and metalloproteinase with thrombospondin motif (ADAMTSs) as well as matrix metalloproteinases (MMPs) are found to be upregulated in OA joints (1-5) and directly involved in OA pathophysiology (6, 7). Therefore, inhibition of these metalloproteinases is potentially a route in which pharmaceutical agents could be designed to retard, suppress and even halt the progression of OA development. However, broad spectrum inhibitors of MMPs, which were shown to be chondro-protective in animal models, raised safety concerns in clinical trial, pinpointing a need for inhibitors with greater specificity (8). The loss of the key catabolic enzyme activity, such as ADAMTS-5, protects C57/BL6 mice from OA lesions (9-11) compared with ADAMTS-1 or -4 deletion, suggesting that ADAMTS-5 plays a central role in surgically-induced and inflammatory mouse models (12, 13). However, more recent data suggests that another aggrecanase, not yet determined, cleaves aggrecan before its secretion. Moreover, a non-catalytic function of ADAMTS-5 is suggested to have competitive interactions between major endocytic recycling machinery (14).

As a model for human OA, STR/Ort mice have proved that genetic susceptibility is a solid basis for assessing the protection afforded by novel treatment (15, 16). Crucially, STR/Ort mouse OA closely resembles human OA and progresses to cartilage loss, along with similar alterations in bone

mass and structure (17-20). Pertinently, it has been shown that the OA-related proteoglycan depletion observed predominantly across the medial tibial compartment in STR/Ort mouse joints also likely involves both collagenase and aggrecanase activities, as in the human (20, 21). Interestingly, female STR/Ort mice also have a high bone mass versus C57/BL6, with bone marrow compression and extramedullary haematopoiesis observed by 36-weeks of age (22). Consistently, recent studies from our group showed that this difference is present even in young STR/Ort mice, which have increased cortical and trabecular parameters in comparison to age-matched CBA mice (23). These characteristics make the STR/Ort strain an intriguing and hitherto unexplored target, in which to explore potentially protective transgenic strategies.

TIMP-3 (Tissue Inhibitor of Matrix Metalloproteinases-3) is a native biological inhibitor of enzyme activity for members of the metzincin family, including collagenases (MMP-1, -8 and -13), gelatinases (MMP-2 and -9) and aggrecanases (ADAMTS-4 and -5). Extracellular trafficking of TIMP-3 is regulated by the competition between ECM binding and endocytosis via low density lipoprotein receptor-related protein 1 (LRP-1) (24-26). It has previously been shown that modifications in TIMP-3 expression could modify joint degeneration (27) and that loss/gain of TIMP-3 function leads to significant alteration in bone structure (28, 29). Herein, we have used a variant of TIMP-3, named [1A]TIMP-3 harbouring a single alanine addition to the amino-terminal end, which was shown to inhibit aggrecanases, namely ADAMTS-4/5, with much greater selectivity than other MMPs (30, 31). This modified activity is driven by conformational changes, where the active site is tilted and the interaction of Phe³⁴ of the inhibitor with MMPs is lost (31).

Our aim was to assess the potential aggrecanase selectivity of [-1A]TIMP-3 on spontaneous OA development and bone formation in STR/Ort mice. We found that high levels of [-1A]TIMP-3 expression in transgenic STR/Ort mice can effectively attenuate cartilage destruction and OA-related subchondral thickening, but, strikingly, also significantly augment bone mass.

MATERIALS AND METHODS

Generation of Lentiviral and plasmid vectors to overexpress [-1A]TIMP-3.

The lentivirus vector was constructed by cloning [-1A]TIMP-3 with a FLAG tag into the EcoRV-Sall site of the pCCL expressing vector driven by elongation factor 1a (EF1a) promoter. The construct also contained growth factor receptor (NGFR) as a marker (Figure 1A).

293T17 cells were co-transfected with transfer vector and packaging vectors by electroporation using the Neon™ transfection system (Invitrogen, UK) to produce the virus. Viral supernatants were harvested 48 and 72 h after transfection and concentrated by ultracentrifugation at 10,000 g for 2 h. The viral pellet was collected and dissolved in PBS.

A second conditional plasmid was generated using Col2a1 3kb promoter and 3k first intron that drives specific expression in chondrocytes (32). The [-1A]TIMP-3 cDNA was followed by an IRES and beta-galactosidase reporter gene (Figure 1B).

Transient transduction was performed at 10 multiplicity of infection (MOI) units in two cell lines, HEK293 and HTB94, to test integration efficacy and overexpression capacity. Flow cytometry with anti-NGFR conjugated APC was used to estimate transfection efficiency. Trichloroacetic acid (TCA) protein precipitation and western blot were used to test [-1A]TIMP-3 protein levels.

Animals

STR/Ort mouse colony maintained at the Royal Veterinary College, London was used to generate transgenic mice overexpressing [-1A]TIMP-3 in this background. Each fertilised embryo was injected with either Col2a1[-1A]TIMP-3 linearized plasmid in male pro nucleus or by infection using 100 lentiviral particles (EF1a[-1A]TIMP-3) per embryo. The latter procedure was also used to generate transgenic mice in control CBA strain (EF1a[-1A]TIMP-3 CBA). Newly born transgenic mice were routinely genotyped by qPCR using reporter gene LacZ as well as the [-1A]TIMP-3 insert (Supplementary Table 1). All experimental protocols were performed in compliance with the UK Animals (Scientific Procedures) Act 1986 regulations.

We analysed hind limb bones and knee joints isolated from the STR/Ort mice at 40 weeks of age. Age-matched non-transgenic (untreated) STR/Ort or transgenic CBA, a parental background strain of the STR/Ort mice were used as controls. The exact number of animals used in each analysis is described in Supplementary Table 2.

Western blotting

Cultured media from transfected HEK293 and HTB94 cells were precipitated with TCA, resuspended in PBS to equal total protein content, resolved by 10% SDS-PAGE under reducing conditions, and electrotransferred to Hybond P[®] polyvinylidene difluoride (PVDF) membranes (Amersham Biosciences, Little Chalfont, UK). Membranes were blocked with 5% skimmed milk and probed overnight at 4°C with rabbit polyclonal anti-TIMP-3 antibody (1:2000 dilution, AB6000, Millipore, UK), followed by incubation with horseradish peroxidase-labeled goat anti-rabbit antibody (1:10,000 dilution, DAKO, Japan). Analysis was performed using the ECL Advanced Western Blotting Detection Kit (Amersham Biosciences). For western blots using mouse tails, 250mg of tissue was boiled at 95°C for 10min in Laemmli buffer and samples were electrophoresed in 4-12% Bis-Tris precast gels

(NuPAGE) at 200V for 35min. Proteins were transferred on PVDF membranes, blocked and incubated overnight with either anti-TIMP-3 antibody or rabbit anti-beta actin (ab8227, Abcam, UK). Detection was performed using fluorescent goat anti-rabbit secondary antibodies (IRDye 680RD for actin and 800CW for TIMP-3, Licor Inc, USA) and relative quantitation was conducted with beta-actin as a reference protein.

Quantitative polymerase chain reaction (qPCR)

Integration of [-1A]TIMP-3 cDNA and overexpression were monitored by qPCR at both genomic DNA and mRNA levels (details in Supplementary Methods).

Micro-computed tomography (μ CT)

Left and right hind limbs of all STR/Ort mice were dissected and immediately scanned using a Skyscan 1272 μ CT scanner (Bruker, Kontich, Belgium) at 50 kV, 0.5 aluminium filter, 200 mA, voxel size 9.00 μ m and 0.3° rotation angle). Datasets were reconstructed using NRecon and 3D volumes of interest (VOI) were selected using Dataviewer and CTAn software. Morphometric parameters were analysed for tibial metaphyseal trabecular bone, cortical bone in diaphysis and subchondral bone in epiphysis as previously described (33, 34) (details in Supplementary Methods).

***In vitro* bone cell culture and mineralisation assay**

STR/Ort and CBA-mice derived primary osteoblasts were isolated and their mineralisation capacity was assessed by Alizarin Red S (ARS) staining after 4 weeks. To assess the *in vitro* osteo-regulatory effect of [-1A]TIMP-3, osteoblasts were isolated from skeletally mature 12-week old wild-type C57/BL6 mice and infected with [-1A]TIMP-3 or TIMP-3 lentiviruses while untreated and lentivirus-

© 2018 The Authors Arthritis & Rheumatology published by Wiley Periodicals, Inc. on behalf of American College of Rheumatology

mock infected osteoblasts served as controls. , early mineralisation capacity of the infected OBs was evaluated with ARS staining after 21 days (details in Supplementary Methods).

Evaluation of cartilage lesion in STR/Ort mice by histology

Following μ CT, knee joints from all STR/Ort mice were fixed in 4% PFA solution for 24 h, decalcified in 10% EDTA for 3 weeks and subsequently stored in 70% EtOH until processing. Samples were embedded in paraffin wax and sectioned coronally (5 μ m thickness) through the entire joint. Proteoglycan loss was evaluated using Safranin-O/Fast green staining and a validated scoring system following the OARSI recommendations (35). Joints were scored “blinded” by two experienced investigators and scores averaged using a modification to the methods of Poulet *et al.* (18). To obtain robust results, as OA affects predominantly the medial compartment of the tibial plateau (MTP) and femoral condyle (MFC), the average of the maximal scores at both sites was used for each sample. Mean scores were calculated as the average of the scores recorded at eight levels at 90 μ m intervals across the entire joint.

Immunohistochemistry (IHC)

For IHC experiments, sections were deparaffinised, rehydrated and probed with selected antibodies. 2% Normal Goat Serum (NGS) was used for blocking. For [-1A]TIMP-3 detection, an additional step of antigen retrieval was applied by incubation with chondroitinase ABC (Sigma, UK) at 0.01 units/ml. Rabbit anti-mouse TIMP-3 polyclonal antibody against the C-terminus of TIMP-3 (Millipore, UK) was used at 1:3000 dilution in NGS. Rabbit anti-mouse anti-NVTEGE antibody (1:850) was used for ADAMTS-generated neopeptide detection, provided by J. Mort (36). Non-immune rabbit serum served as negative control. Primary antibodies were detected using the Vectastain ABC kit with a secondary goat anti-rabbit biotinylated antibody (Vectorlabs, UK) and visualised with HRP-conjugated streptavidin using 3,3'-diaminobenzidine (DAB).

Statistical analysis

All data were analysed with GraphPad Prism 6 (San Diego, CA) and expressed as mean \pm SD. Data sets were tested for Gaussian distribution with the D'Agostino-Pearson normality test. Comparisons between three or more groups were performed by one-way ANOVA followed by Tukey's multiple comparisons post-hoc test. Mann-Whitney U test or two-tailed Student's t-test were used to compare two groups. Correlations were performed with Pearson's test. In all cases, $p < 0.05$ was considered statistically significant.

RESULTS

In vitro efficacy of [-1A]TIMP-3 lentiviral transduction

In order to evaluate efficacy of lentiviral transduction, we infected the human embryonic kidney cell line (HEK293) as well as the chondrosarcoma HTB94 cell line with a lentiviral construct (Figure 1A). Approximately 75% of HTB94 cells transduced with the [-1A]TIMP-3-containing vector expressed the NGFR marker, which is co-expressed by the same vector; by comparison there was no detectible NGFR marker expression in non-infected control HTB94 cells (Figure 1C).

Western blot analysis showed that control HTB94 cells transduced by empty lentiviral vector secreted a small amount of endogenous TIMP-3 protein into the medium, detected by the anti-TIMP-3 antibody. In contrast, a high level of [-1A]TIMP-3 protein was secreted by HTB94 cells infected with EF1a[-1A]TIMP-3 lentivirus compared with lower level of protein from HEK293 cells (Figure 1D). The data demonstrate effective lentivirus transduction into different types of cells and overexpression of the [-1A]TIMP-3 transgene in chondrocytes.

[-1A]TIMP-3 transgenic overexpression in mice

We generated several transgenic lines using two different methods. The lentivirus-induced global [-1A]TIMP-3 transgenic mice (EF1a[-1A]TIMP-3) were compared with Col2a1[-1A]TIMP-3. The pronuclear injection method of fertilized STR/Ort eggs using Col2a1[-1A]TIMP-3 resulted in low level of integration of the transgene as determined by qPCR of genomic DNA from ear notches (Figure 1E). In order to determine mRNA expression levels within the STR/Ort transgenic mice, total RNA was extracted from whole mouse femoral heads. qPCR using specific primer for FLAG-tag at the 3'end of [-1A]TIMP-3 to distinguish endogenous from transgenic mRNA resulted in a range of mRNA overexpression, ranging between ≤ 2 - and 13-fold increase (Figure 1F). Most of the high expressers were generated from lentiviral infection. [-1A]TIMP-3 mRNA levels were consistent across paired, left and right femoral heads in both EF1a[-1A]TIMP-3 and Col2a1[-1A]TIMP-3 transgenic groups of mice (not shown) but lower levels of expression were noted in the males, especially in those of the Col2a1[-1A]TIMP-3 group, perhaps because of smaller group size, compared to females (Figure 1G). Western blot showed undetectable [-1A]TIMP-3 protein levels in WT and low expressers but between 5-10 fold greater levels in those mice deemed high expressers based upon an assessment of their [-1A]TIMP-3 mRNA levels (Figure 1H). Overall, STR/Ort background transgenic mice were harder to achieve by direct pronuclear injection as fewer eggs were fertilized compared with CBA control and significant number of injected eggs did not survive. Importantly, the various levels of transgene expression achieved, allowed us to determine the "threshold" expression level of [-1A]TIMP-3 needed for effective amelioration of the STR/Ort phenotype.

[-1A]TIMP-3 protects the STR/Ort mice from OA cartilage degradation.

The main OA features in STR/Ort mouse knee are cartilage loss on the MTP and MFC accompanied by osteophyte development and subchondral bone sclerosis (23). Therefore, we investigated these regions at 40 weeks of age using OARSI maximum and mean OA score (Figure 2 A-E). We found that whilst knees of untreated STR/Ort mice at 40 weeks of age had severe loss of the articular cartilage at the MTP and MFC (Figure 2A), STR/Ort transgenic mice over-expressing [-1A]TIMP-3 with either EF1a[-1A]TIMP-3 or Col2a1[-1A]TIMP-3 maintained their articular cartilage (Figure 2B, C). The overall analysis showed a significant reduction or prevention in articular cartilage degradation with a decrease of 57% (mean maximum score 1.4, $p < 0.0001$) for the EF1a[-1A]TIMP-3 group and 22% for Col2a1[-1A]TIMP-3 (mean maximum score 2.5, $p = 0.0165$), as compared to untreated STR/Ort mice (mean maximum score 3.2) (Figure 2D). Similarly, mean scores at the medial sites for both overexpressing STR/Ort groups were significantly lower than in the untreated group (Figure 2E, $p = 0.005$ for EF1a[-1A]TIMP-3 and $p = 0.043$ for Col2a1[-1A]TIMP-3). Furthermore, there is a negative correlation between maximum OA score and [-1A]TIMP-3 expression levels, indicative of a protective effect of the [-1A]TIMP-3 when it is expressed at high levels (Figure 2F, G). A careful examination of stained sections revealed that [-1A]TIMP-3 high-expressers also show signs of reduced proteoglycan accumulation in the cruciate ligaments, restored medial collateral ligament physiology, ameliorated osteophyte formation and abolished synovial activation and inflammatory cells infiltration, which are known hallmarks of OA in this strain (Supplementary Figure 1).

The μ CT data showed that untreated STR/Ort controls suffered from severe subchondral sclerosis on the medial side of the knee joint (Figure 2H, K). This subchondral bone thickening was abrogated in both EF1a[-1A]TIMP-3 and Col2a1[-1A]TIMP-3 transgenic STR/Ort mice (Figure 2 I, J, K).

Localisation of [-1A]TIMP-3 and inhibition of aggrecanases in rescued cartilage

To validate whether the reduction in articular cartilage degradation and diminished aggrecanase cleavage is linked directly to overexpression of [-1A]TIMP-3, immunohistological labelling for [-1A]TIMP-3 and the aggrecan NVTEGE neoepitope was done on adjacent knee joint sections. Figure 3A shows a representative coronal section of protected knee joint from STR/Ort mice in which [-1A]TIMP-3 immunostaining was seen in the adjacent section; [-1A]TIMP-3 is evident in both menisci and articular cartilage (Figure 3B) and resembles the endogenous TIMP-3 localisation with pericellular distribution, as previously described (37).

Immunostaining against the NVTEGE neoepitope, an ADAMTSs-catabolic product, revealed that the medial side in the low-expresser transgenic, OA-prone STR/Ort mouse joints (Figure 3F) show little, if any, labelling for the NVTEGE epitope due to the extensive cartilage damage (verified by Safranin O staining, Figure 3D) and likely loss of known matrix binding partners for this antigen. This is consistent with positive NVTEGE labelling (arrows in Figure 3F) in the apparently intact sites directly neighbouring this damaged OA cartilage tissue, into which OA development is likely actively advancing. The lateral compartment, which is OA-resistant even in the STR/Ort strain, retains relatively intact cartilage, compared with the medial side, yet likely already exhibits slight proteoglycan loss (evidenced by the Safranin O staining, Figure 3E) which co-localises with NVTEGE-positive labelling (Figure 3G). In contrast, high-expresser transgenic STR/Ort mice which are protected from OA and, hence, retain intact cartilage on both medial (Figure 3I) and lateral (Figure 3J) knee joint compartments do not show positive NVTEGE labelling (Figure K-M). This is consistent with an [-1A]TIMP-3-related inhibition of ADAMTS-mediated aggrecan degradation.

Selective inhibition of aggrecanases increases bone mass *in vivo*

Given that STR/Ort mice show increased trabecular bone mass, especially female mice (22), we examined bone mass, expressed as percentage trabecular bone volume per tissue volume (%BV/TV), by μ CT in the tibial metaphysis of all overexpressing mice in comparison with untreated STR/Ort and EF1a[-1A]TIMP-3 CBA control mice. In agreement with previous findings, non-transgenic untreated STR/Ort group showed a significantly increased BV/TV as compared with CBA mice (22). Intriguingly, tibial BV/TV was further increased in both the EF1a[-1A]TIMP-3 and Col2a1[-1A]TIMP-3 groups in comparison with the untreated STR/Ort (Figure 4A, representative images in Figure 4E) and this was consistent with the other μ CT trabecular bone parameters (Supplementary Table 3). The extent of this elevation in BV/TV was greater in EF1a[-1A]TIMP-3 mice, presumably due to higher levels of [-1A]TIMP-3 mRNA overexpression. Subgroup analysis of low and high [-1A]TIMP-3 expressing mice, showed a statistically significant increase of BV/TV only in high-expressing STR/Ort mice (Figure 4B). A similar trend was observed in the EF1a[-1A]TIMP-3 CBA mice (Figure 4C).

Data sub-analysis based on gender separation revealed that STR/Ort females of both transgenic mouse lines had substantially higher bone mass than untreated controls (Figure 4D). The difference was greater in EF1a[-1A]TIMP-3 female high-expressers. Male STR/Ort, which expressed relatively lower overall levels of [-1A]TIMP-3, similarly show higher bone mass in the EF1a[-1A]TIMP-3 group compared with untreated STR/Ort mice (Figure 4D). Finally, cortical bone analysis revealed increased mean cortical bone thickness in transgenic STR/Ort mice, demonstrating that the effect of [-1A]TIMP-3 overexpression on bone tissue also extends to cortical bone regions (Figure 4F and G).

[-1A]TIMP-3 enhances *in vitro* bone formation

The next sets of experiments were devised to: i) explore if the increase in bone mass is coupled with sustained changes in osteoblasts isolated from CBA and STR/Ort mice with divergent levels of [-1A]TIMP-3 transgene overexpression; ii) to test whether enhanced bone mass in transgenic mice was related to a developmental programme that was abrogated by aggrecanase inhibition, or are the changes in isolated adult osteoblasts correspond with greater bone formation observed in [-1A]TIMP-3 overexpressing mice. Primary osteoblasts were isolated from long-bones of CBA and STR/Ort EF1a[-1A]TIMP-3 overexpressing mice and the level of mineralisation using ARS staining was assessed. Results showed that the level of mineralisation in isolated osteoblasts is reliant upon the level of [-1A]TIMP-3 expression (Figure 5A and B); higher [-1A]TIMP-3 expression levels in both STR/Ort or CBA were associated with greater extent of mineralisation, forming larger and more numerous bone nodules compared with cells derived from low-expressers.

To further verify whether [-1A]TIMP-3 directly affects osteoblastic bone formation and mineralisation in cells that were not previously exposed to the [-1A]TIMP-3 transgene *in vivo*, we performed *in vitro* transduction of adult osteoblasts, isolated from the long bones of three month old wild-type mice. We found that [-1A]TIMP-3-transduced osteoblasts formed a significantly increased number of mineralised bone nodules compared with untreated or mock infected cells (Figure 5C and D). In order to verify that [-1A]TIMP-3 exerts different effects compared to native, endogenous TIMP-3, we extended the experiments to include TIMP-3. In contrast to transduction with [-1A]TIMP-3, native TIMP-3 completely abrogated bone formation, consistent with our previous *in vivo* findings, where overexpression of Col2a1-driven TIMP-3 resulted in significant reduction of bone mass (28). Similarly, mRNA levels of *Alp*, *Col1a1*, *Ocn* and *Runx-2*, reflecting osteogenic stimulation, were found elevated in [-1A]TIMP-3-transduced osteoblasts and suppressed in TIMP-3 (Figure 5E).

DISCUSSION

The primary aim of our study was to evaluate whether OA that arises spontaneously in STR/Ort mice can be ameliorated by an aggrecanase inhibitor. We utilized [-1A]TIMP-3, a modified TIMP-3 that was shown to be “selective” but not “specific” inhibitor against aggrecanases *in vitro* (30).

We compared knee joints of untreated STR/Ort with STR/Ort mice that were genetically modified to either overexpress [-1A]TIMP-3 specifically in chondrocytes, using Col2a1 promoter/enhancer Col2a1[-1A]TIMP-3, or through ubiquitous lentiviral transduction EF1a[-1A]TIMP-3. The results clearly showed that the overexpression of [-1A]TIMP-3 protects articular cartilage or reduce the severity of cartilage degradation compared with age-matched untreated STR/Ort control mice. This protection was dependent on expression levels of [-1A]TIMP-3. High-expressers of [-1A]TIMP-3 scored low as opposed to low-expressers which obtained higher maximum and mean OA scores in an inversely correlated manner, irrespective of lentiviral or Col2a1-selective delivery. Our findings demonstrate the critical roles of aggrecanases in STR/Ort OA pathophysiology, and highlight that [-1A]TIMP-3 can restrict cartilage aggrecan degradation by blocking aggrecanase activity not only ADAMTS-4 and 5.

Furthermore, our findings indicate that the characteristic subchondral bone sclerosis observed in the medial site of epiphysis (19, 38) was also significantly reduced in response to [-1A]TIMP-3 overexpression. This suggests that [-1A]TIMP-3 may exert a regulatory role in the communication between chondrocytes and bone cells, or indeed have a direct role on bone through chondrocyte transdifferentiation into osteoblasts (39). Alternatively, the possibility that the primary effect of [-1A]TIMP-3 could lead to reduced subchondral bone sclerosis which, in turn, improves cartilage stability needs to be further explored.

It should be noted that catabolic enzymes such as ADAMTS-4 and 5 are endocytosed by chondrocytes via LRP-1 (25, 40) which potentially provides protection for cartilage. It is also notable that LRP-1-mediated endocytic clearance of TIMP-3 (37, 41) and [-1A]TIMP-3 is also likely to be regulated by LRP-1 (42). This is evident when sulphated glycans (37) inhibited binding of TIMP-3 to LRP-1 or mutants of LRP-1 binding inhibited metalloproteinase-mediated degradation of cartilage at lower concentrations and for longer than wild-type TIMP-3, indicating that their increased half-lives improved their ability to protect cartilage (42).

The fact that endogenous level of TIMP-3 could be very tightly regulated by LRP-1 at steady state requires an overexpression system rather than KO to investigate role of TIMP-3 in vivo, as in this study where a significant amount of [-1A]TIMP-3 protein in high-expressers group was evident by western blot, compared to endogenous TIMP-3 in wild-type. This indicates that overexpression system overcome LRP-1-mediated endocytic clearance. However, in OA cartilage and under inflammatory conditions this clearance system is impaired due to increased shedding of LRP-1 (26). It is plausible that LRP-1 shedding, defective LRP-1 clearance, or the apparent role of GLUT4/LRP-1 interaction (14) may be important contributors to the many defects that increase the chances of OA development in STR/Ort mice, but we have not investigated this process. Nonetheless, selective aggrecanase inhibitor, [-1A]TIMP-3, is able to ameliorate the cartilage pathology of these mice.

The second major and surprising finding is related to the effect of [-1A]TIMP-3-mediated aggrecanase inhibition on bone mass. STR/Ort mice have an inherent high bone mass phenotype, which is linked to increased osteoblast numbers and bone formation, and reduced osteoclast activity (22). Moreover, STR/Ort females exhibit higher bone mass than males, underlying the reported sexual dimorphism in this strain (19, 43). Evidence presented here show that STR/Ort [-1A]TIMP-3 high-expressers, especially females, had significantly increased trabecular parameters and cortical bone thickness, compared with control and low expresser groups. We expected the opposite effect since our previous studies have demonstrated that high levels of wild-type TIMP-3 overexpression in mouse cartilage lead to lack of secondary ossification and intermediate levels of TIMP-3 had reduced

© 2018 The Authors Arthritis & Rheumatology published by Wiley Periodicals, Inc. on behalf of American College of Rheumatology

bone mass (28). It has already been shown that MMP deficiency e.g. MMP-9 and MT1-MMP deficiencies, can lead to developmental skeletal abnormalities (44, 45). The increased bone mass in STR/Ort mice was mirrored in CBA control mice, which suggests that bone augmentation by [-1A]TIMP-3 is not specific to the STR/Ort strain alone. Taken together, the data suggest that there might be a unique involvement of aggrecanases in bone metabolism and highlight that maintaining skeletal homeostasis depends on balanced matrix remodelling by aggrecanases and collagenases.

The findings of *in vitro* primary osteoblast mineralisation assays show that osteoblasts isolated from highly overexpressing STR/Ort mice had a higher bone-forming capacity. This suggests that bone formation is positively influenced by inhibition of aggrecanases which warrant further investigation. Most importantly, this observation was not strain-specific as *in vitro* infection of wild-type osteoblasts from young C57/BL6 mice also resulted in enhanced bone mineralisation and induction of osteogenic pathways when transduced by lentivirus overexpressing [-1A]TIMP-3 compared with TIMP-3. Our data suggest that [-1A]TIMP-3 may serve as a novel therapeutic agent in osteoporotic bone loss; a notion supported by findings indicating that conditional overexpression of bone-driven TIMP-1, an MMP only inhibitor, in osteoblasts leads to low bone turnover, only in females (46).

In conclusion, the spontaneous OA that develops over time in STR/ort mouse is driven by aggrecanases and [-1A]TIMP-3 overexpression can protect against cartilage damage and subchondral bone thickening in this mouse model. In addition, high levels of [-1A]TIMP-3 overexpression also led to significant increase in bone mass, which highlights a possible dual role of this molecule as a regulator of cartilage and bone homeostasis. In the absence of an effective OA treatment our novel data show that [-1A]TIMP-3 or other similar molecules exhibiting selective affinity for aggrecanases could be strong candidates for OA and osteoporosis treatment.

Acknowledgement

This work was funded by ARUK grant 20039. The authors are grateful to Professor Hideaki Nagase for providing the cDNA for the [-1A]TIMP-3. No other disclosure.

REFERENCES

1. Neuhold LA, Killar L, Zhao W, Sung ML, Warner L, Kulik J, et al. Postnatal expression in hyaline cartilage of constitutively active human collagenase-3 (MMP-13) induces osteoarthritis in mice. *J Clin Invest*. 2001;107(1):35-44.
2. Fuchs S, Skwara A, Bloch M, Dankbar B. Differential induction and regulation of matrix metalloproteinases in osteoarthritic tissue and fluid synovial fibroblasts. *Osteoarthritis Cartilage*. 2004;12(5):409-18.
3. Yang CY, Chanalaris A, Troeberg L. ADAMTS and ADAM metalloproteinases in osteoarthritis - looking beyond the 'usual suspects'. *Osteoarthritis Cartilage*. 2017;25(7):1000-9.
4. Verma P, Dalal K. ADAMTS-4 and ADAMTS-5: key enzymes in osteoarthritis. *J Cell Biochem*. 2011;112(12):3507-14.
5. Echtermeyer F, Bertrand J, Dreier R, Meinecke I, Neugebauer K, Fuerst M, et al. Syndecan-4 regulates ADAMTS-5 activation and cartilage breakdown in osteoarthritis. *Nat Med*. 2009;15(9):1072-6.
6. Glyn-Jones S, Palmer AJ, Agricola R, Price AJ, Vincent TL, Weinans H, et al. Osteoarthritis. *Lancet*. 2015;386(9991):376-87.
7. Nagase H, Kashiwagi M. Aggrecanases and cartilage matrix degradation. *Arthritis Res Ther*. 2003;5(2):94-103.
8. Nemunaitis J, Poole C, Primrose J, Rosemurgy A, Malfetano J, Brown P, et al. Combined analysis of studies of the effects of the matrix metalloproteinase inhibitor marimastat on serum tumor markers in advanced cancer: selection of a biologically active and tolerable dose for longer-term studies. *Clin Cancer Res*. 1998;4(5):1101-9.

9. Glasson SS, Askew R, Sheppard B, Carito B, Blanchet T, Ma HL, et al. Deletion of active ADAMTS5 prevents cartilage degradation in a murine model of osteoarthritis. *Nature*. 2005;434(7033):644-8.
10. Stanton H, Rogerson FM, East CJ, Golub SB, Lawlor KE, Meeker CT, et al. ADAMTS5 is the major aggrecanase in mouse cartilage in vivo and in vitro. *Nature*. 2005;434(7033):648-52.
11. Botter SM, Glasson SS, Hopkins B, Clockaerts S, Weinans H, van Leeuwen JP, et al. ADAMTS5^{-/-} mice have less subchondral bone changes after induction of osteoarthritis through surgical instability: implications for a link between cartilage and subchondral bone changes. *Osteoarthritis Cartilage*. 2009;17(5):636-45.
12. Glasson SS, Askew R, Sheppard B, Carito BA, Blanchet T, Ma HL, et al. Characterization of and osteoarthritis susceptibility in ADAMTS-4-knockout mice. *Arthritis Rheum*. 2004;50(8):2547-58.
13. Little CB, Mittaz L, Belluoccio D, Rogerson FM, Campbell IK, Meeker CT, et al. ADAMTS-1-knockout mice do not exhibit abnormalities in aggrecan turnover in vitro or in vivo. *Arthritis Rheum*. 2005;52(5):1461-72.
14. Gorski DJ, Xiao W, Li J, Luo W, Lauer M, Kisiday J, et al. Deletion of ADAMTS5 does not affect aggrecan or versican degradation but promotes glucose uptake and proteoglycan synthesis in murine adipose derived stromal cells. *Matrix Biol*. 2015;47:66-84.
15. Brewster M, Lewis EJ, Wilson KL, Greenham AK, Bottomley KM. Ro 32-3555, an orally active collagenase selective inhibitor, prevents structural damage in the STR/ORT mouse model of osteoarthritis. *Arthritis Rheum*. 1998;41(9):1639-44.
16. Chiusaroli R, Visentini M, Galimberti C, Casseler C, Mennuni L, Covaceuszach S, et al. Targeting of ADAMTS5's ancillary domain with the recombinant mAb CRB0017 ameliorates disease progression in a spontaneous murine model of osteoarthritis. *Osteoarthritis Cartilage*. 2013;21(11):1807-10.
17. Mason RM, Chambers MG, Flannelly J, Gaffen JD, Dudhia J, Bayliss MT. The STR/ort mouse and its use as a model of osteoarthritis. *Osteoarthritis Cartilage*. 2001;9(2):85-91.
18. Poulet B, Ulici V, Stone TC, Pead M, Gburcik V, Constantinou E, et al. Time-series transcriptional profiling yields new perspectives on susceptibility to murine osteoarthritis. *Arthritis*

Rheum. 2012;64(10):3256-66.

19. Staines KA, Poulet B, Wentworth DN, Pitsillides AA. The STR/ort mouse model of spontaneous osteoarthritis - an update. *Osteoarthritis Cartilage*. 2017;25(6):802-8.

20. Chambers MG, Cox L, Chong L, Suri N, Cover P, Bayliss MT, et al. Matrix metalloproteinases and aggrecanases cleave aggrecan in different zones of normal cartilage but colocalize in the development of osteoarthritic lesions in STR/ort mice. *Arthritis Rheum*. 2001;44(6):1455-65.

21. Flannelly J, Chambers MG, Dudhia J, Hembry RM, Murphy G, Mason RM, et al. Metalloproteinase and tissue inhibitor of metalloproteinase expression in the murine STR/ort model of osteoarthritis. *Osteoarthritis Cartilage*. 2002;10(9):722-33.

22. Pasold J, Engelmann R, Keller J, Joost S, Marshall RP, Frerich B, et al. High bone mass in the STR/ort mouse results from increased bone formation and impaired bone resorption and is associated with extramedullary hematopoiesis. *J Bone Miner Metab*. 2013;31(1):71-81.

23. Staines KA, Madi K, Mirczuk SM, Parker S, Burleigh A, Poulet B, et al. Endochondral Growth Defect and Deployment of Transient Chondrocyte Behaviors Underlie Osteoarthritis Onset in a Natural Murine Model. *Arthritis Rheumatol*. 2016;68(4):880-91.

24. Scilabra SD, Yamamoto K, Pignoni M, Sakamoto K, Muller SA, Papadopoulou A, et al. Dissecting the interaction between tissue inhibitor of metalloproteinases-3 (TIMP-3) and low density lipoprotein receptor-related protein-1 (LRP-1): Development of a "TRAP" to increase levels of TIMP-3 in the tissue. *Matrix Biol*. 2017;59:69-79.

25. Yamamoto K, Troeberg L, Scilabra SD, Pelosi M, Murphy CL, Strickland DK, et al. LRP-1-mediated endocytosis regulates extracellular activity of ADAMTS-5 in articular cartilage. *FASEB J*. 2013;27(2):511-21.

26. Yamamoto K, Santamaria S, Botkjaer KA, Dudhia J, Troeberg L, Itoh Y, et al. Inhibition of Shedding of Low-Density Lipoprotein Receptor-Related Protein 1 Reverses Cartilage Matrix Degradation in Osteoarthritis. *Arthritis Rheumatol*. 2017;69(6):1246-56.

27. Sahebjam S, Khokha R, Mort JS. Increased collagen and aggrecan degradation with age in the joints of *Timp3*(^{-/-}) mice. *Arthritis Rheum*. 2007;56(3):905-9.

28. Poulet B, Liu K, Plumb D, Vo P, Shah M, Staines K, et al. Overexpression of TIMP-3 in Chondrocytes Produces Transient Reduction in Growth Plate Length but Permanently Reduces Adult Bone Quality and Quantity. *PLoS One*. 2016;11(12):e0167971.
29. Javaheri B, Hopkinson M, Poulet B, Pollard AS, Shefelbine SJ, Chang YM, et al. Deficiency and Also Transgenic Overexpression of Timp-3 Both Lead to Compromised Bone Mass and Architecture In Vivo. *PLoS One*. 2016;11(8):e0159657.
30. Wei S, Kashiwagi M, Kota S, Xie Z, Nagase H, Brew K. Reactive site mutations in tissue inhibitor of metalloproteinase-3 disrupt inhibition of matrix metalloproteinases but not tumor necrosis factor-alpha-converting enzyme. *J Biol Chem*. 2005;280(38):32877-82.
31. Lim NH, Kashiwagi M, Visse R, Jones J, Enghild JJ, Brew K, et al. Reactive-site mutants of N-TIMP-3 that selectively inhibit ADAMTS-4 and ADAMTS-5: biological and structural implications. *Biochem J*. 2010;431(1):113-22.
32. Zhou G, Garofalo S, Mukhopadhyay K, Lefebvre V, Smith CN, Eberspaecher H, et al. A 182 bp fragment of the mouse pro alpha 1(II) collagen gene is sufficient to direct chondrocyte expression in transgenic mice. *J Cell Sci*. 1995;108 (Pt 12):3677-84.
33. van 't Hof RJ. Analysis of bone architecture in rodents using microcomputed tomography. *Methods Mol Biol*. 2012;816:461-76.
34. Huesa C, Ortiz AC, Dunning L, McGavin L, Bennett L, McIntosh K, et al. Proteinase-activated receptor 2 modulates OA-related pain, cartilage and bone pathology. *Ann Rheum Dis*. 2016;75(11):1989-97.
35. Glasson SS, Chambers MG, Van Den Berg WB, Little CB. The OARSI histopathology initiative - recommendations for histological assessments of osteoarthritis in the mouse. *Osteoarthritis Cartilage*. 2010;18 Suppl 3:S17-23.
36. Mort JS, Roughley PJ. Production of antibodies against degradative neoepitopes in aggrecan. *Methods Mol Med*. 2004;100:237-50.
37. Troeberg L, Lazenbatt C, Anower EKMF, Freeman C, Federov O, Habuchi H, et al. Sulfated glycosaminoglycans control the extracellular trafficking and the activity of the metalloprotease inhibitor TIMP-3. *Chem Biol*. 2014;21(10):1300-9.

38. Stok KS, Pelled G, Zilberman Y, Kallai I, Goldhahn J, Gazit D, et al. Revealing the interplay of bone and cartilage in osteoarthritis through multimodal imaging of murine joints. *Bone*. 2009;45(3):414-22.
39. Javaheri B, Caetano-Silva SP, Kanakis I, Bou-Gharios G, Pitsillides AA. The Chondro- Osseous Continuum: Is It Possible to Unlock the Potential Assigned Within? *Front Bioeng Biotechnol*. 2018;6:28.
40. Yamamoto K, Owen K, Parker AE, Scilabra SD, Dudhia J, Strickland DK, et al. Low density lipoprotein receptor-related protein 1 (LRP1)-mediated endocytic clearance of a disintegrin and metalloproteinase with thrombospondin motifs-4 (ADAMTS-4): functional differences of non-catalytic domains of ADAMTS-4 and ADAMTS-5 in LRP1 binding. *J Biol Chem*. 2014;289(10):6462-74.
41. Rother S, Samsonov SA, Hempel U, Vogel S, Moeller S, Blaszkiewicz J, et al. Sulfated Hyaluronan Alters the Interaction Profile of TIMP-3 with the Endocytic Receptor LRP-1 Clusters II and IV and Increases the Extracellular TIMP-3 Level of Human Bone Marrow Stromal Cells. *Biomacromolecules*. 2016;17(10):3252-61.
42. Doherty CM, Visse R, Dinakarbandian D, Strickland DK, Nagase H, Troeberg L. Engineered Tissue Inhibitor of Metalloproteinases-3 Variants Resistant to Endocytosis Have Prolonged Chondroprotective Activity. *J Biol Chem*. 2016;291(42):22160-72.
43. Mahr S, Menard J, Krenn V, Muller B. Sexual dimorphism in the osteoarthritis of STR/ort mice may be linked to articular cytokines. *Ann Rheum Dis*. 2003;62(12):1234-7.
44. Engsig MT, Chen QJ, Vu TH, Pedersen AC, Therkildsen B, Lund LR, et al. Matrix metalloproteinase 9 and vascular endothelial growth factor are essential for osteoclast recruitment into developing long bones. *J Cell Biol*. 2000;151(4):879-89.
45. Holmbeck K, Bianco P, Caterina J, Yamada S, Kromer M, Kuznetsov SA, et al. MT1-MMP-deficient mice develop dwarfism, osteopenia, arthritis, and connective tissue disease due to inadequate collagen turnover. *Cell*. 1999;99(1):81-92.

46. Geoffroy V, Marty-Morieux C, Le Goupil N, Clement-Lacroix P, Terraz C, Frain M, et al. In vivo inhibition of osteoblastic metalloproteinases leads to increased trabecular bone mass. *J Bone Miner Res.* 2004;19(5):811-22.

LEGENDS TO FIGURES

Figure 1. Evaluation of lentiviral expression. Illustrations of the constructed vectors for the [-1A]TIMP-3 overexpression with lentivirus (LV)-driven EF1a promoter (A) and conditional Col2a1-driven transductions (B). Chondrocytic HTB94 cells, analysed by flow-cytometry, show increased expression of NGFR in cells expressing the lentiviral transgene (C). Western blots (D) of HTB94 cells showed small quantities of endogenous TIMP-3 in lentiviral empty vector (LV-empty) as compared to high protein levels in both 293 and HTB94 [-1A]TIMP-3 overexpressing cells (LV-[-1A]TIMP-3). Integration of [-1A]TIMP-3 into genomic DNA, extracted from ear notches of all mice, was evaluated by qPCR showing that [-1A]TIMP-3 STR/Ort low expressers, especially in the Col2a1[-1A]TIMP-3 group (E), which showed statistical significance, compared with the EF1a[-1A]TIMP-3 CBA mice (E). [-1A]TIMP-3 mRNA quantification in femoral heads showed higher levels of expression in EF1a[-1A]TIMP-3 STR/Ort mice (F). Mice groups were separated into low (open) and high (solid) expressers according to mRNA expression levels with a cut-off value of 2 -fold difference (F). Males expressed lower levels of [-1A]TIMP-3 in both transgene groups, particularly in Col2a1[-1A]TIMP-3 compared with females (G). [-1A]TIMP-3 protein levels were confirmed by western blot showing increasing amount in high-expressers compared with WT and low-expressers (H) ns: not significant, * $p < 0.05$, *** $p < 0.001$, **** $p < 0.0001$.

Figure 2. [-1A]TIMP-3 overexpression protects STR/Ort mice from OA cartilage degradation. Untreated STR/Ort mice at 40 weeks of age show severe OA erosion in the medial sites (M) of tibial plateau and femoral condyles (A), while both EF1a[-1A]TIMP-3 (B) and Col2a1[-1A]TIMP-3 (C) show cartilage protection. High-expresser (green) OA scores of both [-1A]TIMP-3 overexpressing transgenes were significantly lower than age-matched untreated STR/Ort, which had high maximum (D) and mean OA scores (E) of the knee joints. Negative correlations between [-1A]TIMP-3 expression levels and OA scores, with statistical significance was found in both EF1a[-1A]TIMP-3 (F) and Col2a1[-1A]TIMP-3 (G) groups, suggesting that mice with high expression levels (solid) were better protected than low expressers (open). Subchondral bone thickness was assessed by μ CT demonstrating that osteoarthritic untreated STR/Ort mice showed severe sclerotic lesions (arrow) at the medial side of their tibial epiphysis (H) compared with EF1a[-1A]TIMP-3 (I) and Col2a1[-1A]TIMP-3 (J). Quantification of subchondral bone thickness (K) showed significant reduction on the medial (closed) site while the lateral (open) site seems unaffected. * $p < 0.05$; *** $p < 0.001$, **** $p < 0.0001$.

Figure 3. Localisation of [-1A]TIMP-3 and inhibition of aggrecanases activity in articular cartilage. High-expressing mice, which were protected from OA as revealed by Safranin O staining (A) showed immunohistochemical staining for anti-TIMP-3 antibody (B) which indicated that [-1A]TIMP-3 protein was translated at high levels. Rabbit IgG was used as negative control (C). STR/Ort mice expressing low levels of the transgene showed cartilage degradation at the medial site (D), which was concomitant with lack of ADAMTS-derived NVTEGE neoepitope in adjacent section in (F), where arrows indicate peripheral neoepitopes staining in meniscus (m) and cartilage matrix that was not affected yet by proteolysis (F). (E) shows the lateral chondyle and plateau of the same knee in which

© 2018 The Authors Arthritis & Rheumatology published by Wiley Periodicals, Inc. on behalf of American College of Rheumatology

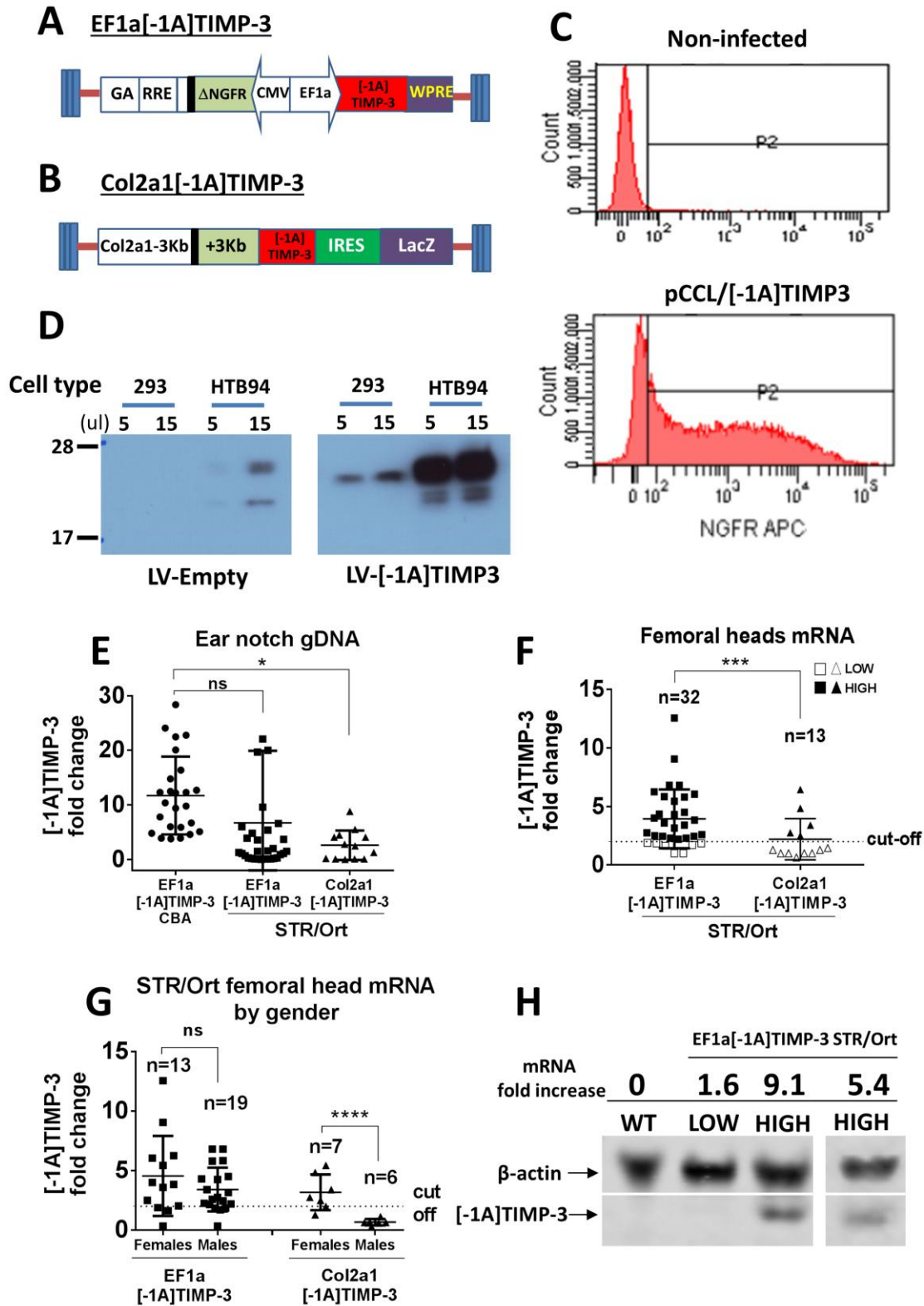
neopeptides immunolabelling were present (G, circled), while rabbit IgG served as negative control (H). In contrast, mice with high expression levels retained cartilage matrix integrity at both medial (I) and lateral (J) sites with undetectable levels of NVTEGE at either sites (K, L) suggesting the inhibition of ADAMTS-4/5 neopeptides by [-1A]TIMP-3. Rabbit IgG was used as negative control (M).

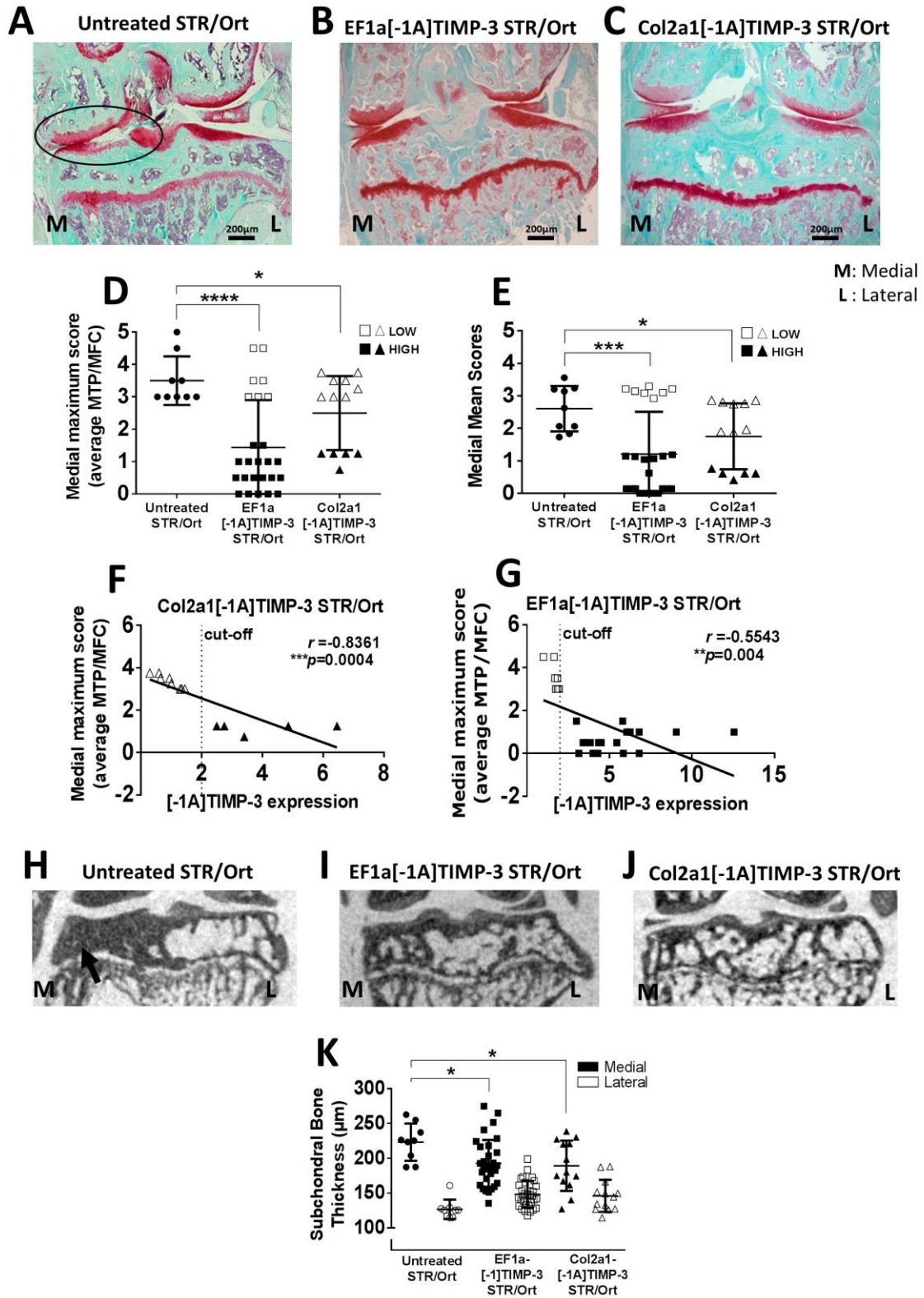
Figure 4. Selective inhibition of aggrecanases by [-1A]TIMP-3 leads to augmented bone

mass *in vivo*. μ CT trabecular analysis showed that untreated STR/Ort mice have significantly increased bone mass as compared to EF1a[-1A]TIMP-3 CBA (A). Both EF1a[-1A]TIMP-3 and Col2a1[-1A]TIMP-3 overexpressing mice had significantly increased bone mass as compared to the untreated STR/Ort mice (A). Elevation of BV/TV was observed only in mice expressing high (solid) levels of [-1A]TIMP-3 STR/Ort, while low (open) did not differ from untreated (B). In (C), the increase in EF1a[-1A]TIMP-3 CBA strain was not significant. Gender analysis showed that STR/Ort females overexpressing either transgene had significantly higher bone mass compared with untreated females (D). STR/Ort overexpressing males showed increase in bone mass only with lentiviral EF1a[-1A]TIMP-3 vector (D). Representative images of the STR/Ort female groups in (E), where red lines show the bone volume of interest (VOI) which was analyzed in this experiment. The same motif was observed by cortical bone measurements of the same female group (F) and represented in (G). ** $p < 0.01$; *** $p < 0.001$, **** $p < 0.0001$ as compared to the untreated STR/Ort, †† $p < 0.01$, ††† $p < 0.0001$ as compared to EF1a[-1A]TIMP-3 CBA.

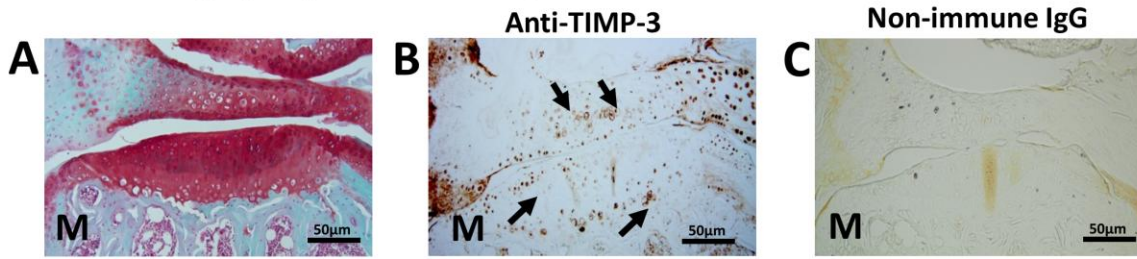
Figure 5. [-1A]TIMP-3 overexpression increases bone formation, both in transgenic mice-derived and newly infected primary osteoblasts. *In vitro* bone mineralisation assay by ARS indicated that long bone osteoblasts derived from high-expressing EF1a[-1A]TIMP-3 STR/Ort and CBA mice had higher bone formation capacity than low-expressing osteoblasts (A), forming more and larger bone nodules with statistically significant percentage of stained area (B) at 28 days of mineralisation. C57/BL6 mature osteoblasts, isolated from young mice, were infected with lentiviral [-1A]TIMP-3 or TIMP-3 and measured for extent of mineralisation at 21days, showing significantly higher rate of mineralisation in the [-1A]TIMP-3 group, compared with untreated or mock osteoblasts (C). In contrast, TIMP-3 overexpression completely stopped mineralisation of bone matrix (C, D and E). The [-1A]TIMP-3 group also showed significant increase in osteogenic gene markers' expression such as alkaline phosphatase (ALP), osteocalcin (OCN), collagen type I (COL1A1) and transcription factor Runx-2 compared with untreated or mock infection (E). ns: not significant, * $p < 0.05$; ** $p < 0.01$; *** $p < 0.001$, **** $p < 0.0001$.

Supplementary Figure 1. OA hallmarks are ameliorated by [-1A]TIMP-3 high-expression in STR/Ort mice. Proteoglycan accumulation is diminished on the cruciate ligament resulting in reduced Safranin O staining in high-expressers as compared to controls (A). In OA joints of the untreated STR/Ort, the medial collateral ligament show increased signs of ossification which leads to hypertrophy. This hallmark is completely diminished in [-1A]TIMP-3 high-expressing mice (B). Similarly, osteophyte formation is abrogated (C) and infiltration of inflammatory cells in the synovium is markedly diminished (D).

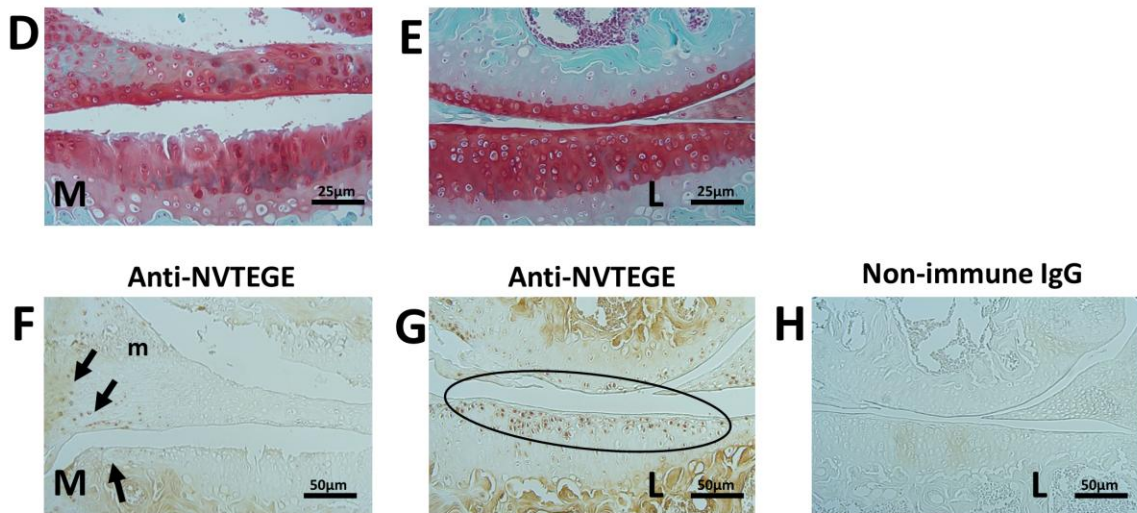




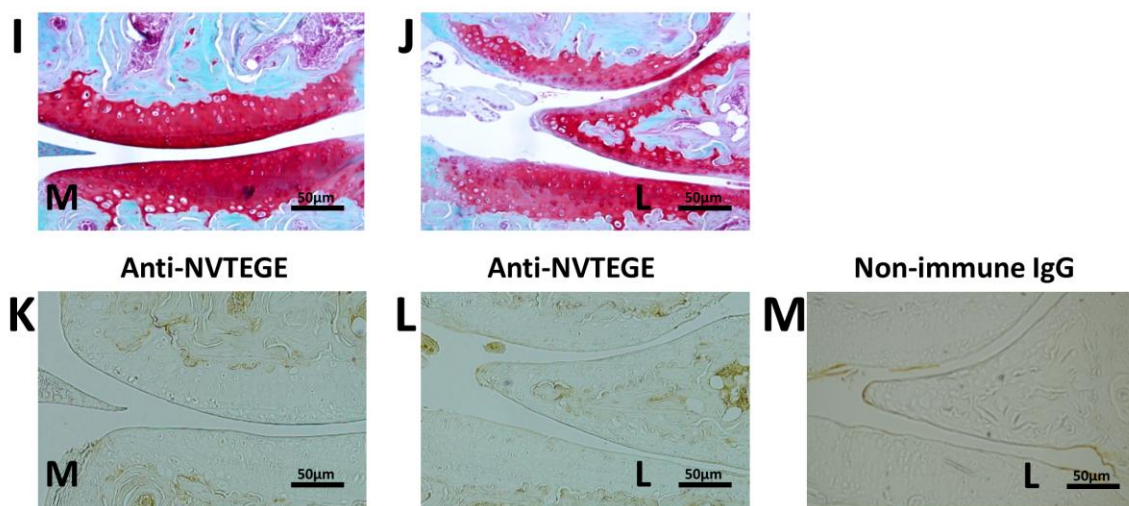
High [-1A]TIMP-3 overexpression



Low [-1A]TIMP-3 overexpression



High [-1A]TIMP-3 overexpression



M: Medial
L: Lateral

